Single-crystal Magnetic Properties of Lanthanide Complexes. Part VI.[1] Hexakis(antipyrine)thulium(III) Tri-iodide

By **M. Gerloch** * and **D. J. Mackey**, University Chemical Laboratories, Lensfield Road, Cambridge CB2 1EW

The principal magnetic moments of crystals of hexakis(antipyrine)thulium(III) tri-iodide (antipyrine is 2,3-dimethyl-1-phenyl-Δ^3-pyrazolin-5-one), have been measured in the temperature range 300—80 K. They are interpreted within a free-ion f^{12}, $^3H_6 + {}^3H_4$, basis perturbed by a crystal field of D_{3d} symmetry. The effects of intermediate coupling on the basis eigenvectors has been included into the crystal-field calculations. Values related to the coefficient of the second-order potential and for the fourth-order radial parameter [$A_2^0\langle r^2\rangle$ and ρ_4, respectively] have been determined. Magnetic moments are not affected by changes in the sixth-order radial integral ρ_6 significantly.

In this series we are studying the principal and average magnetic properties of the trigonally distorted octahedral (D_{3d}) lanthanide complexes Ln(antip)$_6$I$_3$ (antip = antipyrine = 2,3-dimethyl-1-phenyl-Δ^3-pyrazolin-5-one). Throughout, a crystal-field model has been parameterized by the second-, fourth-, and sixth-order radial integrals ρ_2, ρ_4, ρ_6, and the distortion angle θ, this being the effective angle subtended by any M–O bond and the principal, three-fold molecular axis. A more variable feature of the model has been the basis functions used in the calculations. The complete configurational manifolds were used for the f^1 and f^{13} systems but problems of

[1] Part V, M. Gerloch and D. J. Mackey, *J. Chem. Soc.* (*A*), 1971, 3372.

computing time have precluded such comprehensive bases for the many-electron lanthanides. Further, the breakdown of Russell–Saunders coupling evidenced by absorption and fluorescence spectral studies of lanthanide compounds [2] has required the use of basis-state eigenvalues derived from fitting intermediate coupling ' free-ion ' models to the observed spectra. Part V [1] described a further refinement in which the basis eigenvectors used were also derived from the intermediate coupling model. It transpired that this refinement was unnecessary for the computation of magnetic moments. The present paper is concerned with the thulium(III) member of the series, $Tm(antip)_6I_3$, with the f^{12} configuration. It has been known for some time that, for the lower states at least, thulium presents a most

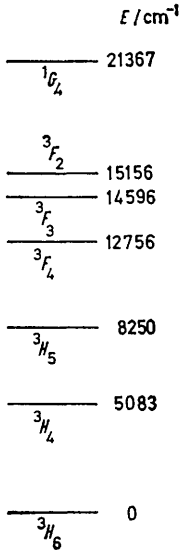

FIGURE 1 Free-ion energy levels for states of thulium(III) below 22,000 cm^{-1} above the ground state

striking example of the breakdown of Russell–Saunders coupling.

Spectra of thulium sulphate, $Tm_2(SO_4)_3,8H_2O$, have been studied by Bethe and Spedding [3] and of thulium ethyl sulphate, $Tm(EtSO_4)_3,9H_2O$, by Gruber and Conway.[4] Bethe and Spedding [3] and Spedding [5] fitted to the experimental observations an intermediate coupling model for the free thulium(III) ion parameterized by one Condon–Shortley interelectron repulsion (i.e.r). parameter F_2, and a spin–orbit coupling coefficient ζ: by use of hydrogenic orbitals, they assumed fixed values for the other i.e.r. parameters from fixed F_2/F_4, F_2/F_6 ratios. Gruber and Conway [4] performed similar calculations for their ethyl sulphate spectra. Runciman and Wybourne [6] have also studied an intermediate coupling model paramatized more freely with F_2, F_4, F_6, and ζ: their calculations also studied the effects of including and neglecting a Trees correction. Figure 1 summarizes the observed or calculated free-ion eigenvalues for thulium(III) states below *ca.* 22,000 cm^{-1} above the ground state. The calculated value for the $^3H_4$ state is based on the parameter values of Runciman and Wybourne which best fit all other observed levels (see Appendix for a discussion of printing errors in ref. 6).

The most obvious feature of the manifold in Figure 1 is the reversal of the $^3H_4$ and $^3H_5$ states with respect to the Landé splitting rule. Such a reversal does not occur [2] elsewhere in the lanthanide(III) term splittings so far as ground terms are concerned. Such obvious breakdown of Russell–Saunders coupling clearly requires us to use appropriate ' intermediate-coupling ' vectors for our basis functions. However, none of the authors concerned with the intermediate coupling problem [3-6] have published eigenvectors. In the Appendix, we reproduce calculated vectors associated with the eigenvalues calculated by Runciman and Wybourne. We note for the immediate discussion the approximate ' purities ' of some states as follows:

' $^3H_6$ ' is 99% pure
' $^3H_4$ ' is 8% $^3H_4$ with 60% $^3F_4$ and 33% $^1G_4$
' $^3H_5$ ' is $^3H_5$ exactly
' $^3F_4$ ' is 31% $^3F_4$ with 53% $^3H_4$ and 16% $^1G_4$

The extensive $^3H_4/^3F_4/^1G_4$ mixing under spin–orbit coupling is clear. An apparently closer approach to the Landé interval rule would appear if we were to interchange the labelling of the $^3H_4$ and $^3F_4$ states. The accepted labelling of these states derives essentially from the conventional approach to state parentage. Whichever labelling scheme is favoured, it is still clear that basis eigenvectors must be those derived from diagonalization of the intermediate coupling matrix. Accordingly our calculations below have used a $^3H_6 + {}^3H_4$ basis, the vectors being those from the intermediate coupling scheme. A selection of final calculations have been checked using as basis all six states below 15,200 cm^{-1} above the ground state. The inclusion of these extra states into the calculations makes only a trivial alteration to the calculated magnetic moments.

EXPERIMENTAL

Powder susceptibilities and crystal anisotropies of $Tm(antip)_6I_3$ were measured in the temperature range 300—80 K by Gouy and Krishnan ' critical torque ' techniques, respectively. Mean susceptibilities and anisotropies have been corrected for the diamagnetic properties of the isomorphous lutetium compound.[7] Procedures, calibrations, and definitions are as in ref. 8. Mean susceptibilities are listed in Table 1, crystal anisotropies in Table 2, and interpolated principal moments in Table 3.

[2] G. H. Dieke and H. M. Crosswhite, *Appl. Optics*, 1963, **2**, 675.
[3] H. A. Bethe and F. H. Spedding, *Phys. Rev.*, 1937, **52**, 454.
[4] J. B. Gruber and J. G. Conway, *J. Chem. Phys.*, 1960, **32**, 1178.
[5] F. H. Spedding, *Phys. Rev.*, 1940, **58**, 255.
[6] W. A. Runciman and B. G. Wybourne, *J. Chem. Phys.*, 1959, **31**, 1149.
[7] M. Gerloch and D. J. Mackey, *J. Chem. Soc.* (*A*), 1970, 3030.
[8] B. N. Figgis, M. Gerloch, J. Lewis, and R. C. Slade, *J. Chem. Soc.* (*A*), 1968, 2021.

TABLE 1

Experimental mean molecular susceptibilities of $Tm(antip)_6I_3$

T/K	$10^6\chi_M'$/ c.g.s.u. mole^{-1}	T/K	$10^6\chi_M'$/ c.g.s.u. mole^{-1}
307·0	22,800	194·5	35,200
295·0	23,600	175·0	38,600
287·0	24,300	160·0	42,300
281·5	24,800	139·0	47,800
272·5	25,400	121·5	53,700
264·0	26,400	109·0	59,700
247·0	28,100	99·5	64,500
232·0	29,900	90·0	70,400
215·5	31,900		

TABLE 2

Experimental molecular anisotropies of $Tm(antip)_6I_3$

T/K	$10^6(\chi_\perp - \chi_\parallel)$/ c.g.s.u. mole^{-1}	T/K	$10^6(\chi_\perp - \chi_\parallel)$/ c.g.s.u. mole^{-1}
293·5	12,800	158·0	38,500
275·0	15,200	144·0	43,700
255·5	17,700	136·0	46,700
233·0	21,000	115·5	58,000
212·5	24,700	99·5	68,500
194·0	29,800	81·5	81,400
172·5	34,000		

TABLE 3

Principal magnetic moments of $Tm(antip)_6I_3$

T/K	$\bar{\mu}$/BM	$\mu_\parallel$/BM	$\mu_\perp$/BM
295·0	7·47	6·00	8·11
287·0	7·47	5·91	8·13
281·5	7·47	5·87	8·16
272·5	7·45	5·80	8·16
264·0	7·47	5·69	8·21
247·0	7·45	5·57	8·25
232·0	7·45	5·40	8·28
215·5	7·42	5·22	8·30
194·5	7·40	5·02	8·33
175·0	7·36	4·78	8·35
160·0	7·36	4·66	8·39
139·0	7·29	4·40	8·37
121·5	7·23	4·19	8·35
109·0	7·22	4·10	8·35
99·5	7·17	3·98	8·32
90·0	7·12	3·85	8·29

DISCUSSION

Energy levels as functions of the trigonal distortion angle θ for the lowest ($^3H_6$) state are shown in Figure 2. There is an A_{1g} ground state always but for the A_{1g} and A_{2g} levels for $\theta > ca.\ 57°$, A_{2g} lies only *ca.* 0·5 cm^{-1} above the ground state. This behaviour is reminiscent of that observed for the terbium (f^8) analogue,[9] except that the close proximity of the A_{1g} and A_{2g} levels there occurred for $\theta < ca.\ 53°$. And as for $Tb(antip)_6I_3$, the opposite sense of distortion leaves an E_g state within *ca.* 80 cm^{-1} of the ground state. The diagram is very complex leaving many levels close to the ground state. One curious feature is the nearly perfect degeneracy of the A_{1g} and A_{2g} levels at the top left of the Figure. These levels are obviously related to those at ground level for the reverse sense of distortion, but do not link up, of course, in the Figure. The overall splitting of the $^3H_4$ state (not shown) is about a quarter of that for the $^3H_6$.

As might be expected from the A_{1g} ground state, when $\theta < \theta_{oct}$, both $\mu_\parallel$ and $\mu_\perp$ tend to vanish apart from a small TIP term. When $\theta > \theta_{oct}$ a high parallel moment, independent of temperature below T *ca.* 100 K, arises from the large matrix element of $\hat{\mu}_\parallel$ between the A_{2g} and A_{1g} levels. There is no matrix element of $\hat{\mu}_\perp$ within this pair of levels, however, so that $\mu_\perp$ tends to zero as temperature is decreased. All this behaviour is similar to that of the terbium congener which was discussed in detail in Part III.

Figure 3 shows calculated principal and mean magnetic moments at 300 and 100 K as functions of the effective distortion angle θ. The sign of anisotropy $\Delta\mu$ is determined by the sign of distortion and is such that $\mu_\parallel < \mu_\perp$ for $\theta < \theta_{oct}$. The mean moments $\bar{\mu}$ vary with θ a little more than for the f^1, f^3, f^8, f^{11}, or f^{13} members of this series, particularly at 100 K, although such variations are still small. However, we also find (not shown) that,

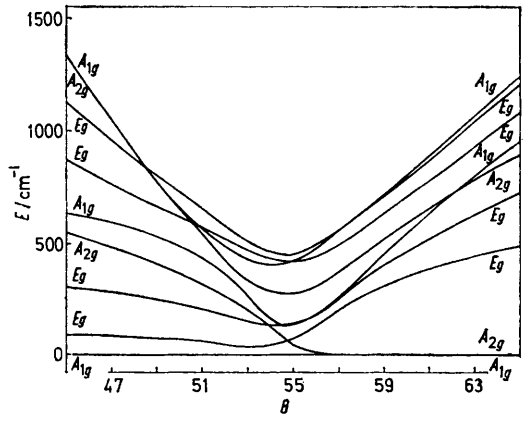

FIGURE 2 Calculated energies of ground-state components for f^{12} in the D_{3d} crystal field; ρ_2 1500, ρ_4 400, and ρ_6 200 cm^{-1}

in common with the above systems, the mean moments at either temperature are still independent of the value of ρ_2, changing by *ca.* 1% as ρ_2 changes from 500 to 2000 cm^{-1}. An interesting feature of the principal moments not previously observed in this series is the crossing of the 300 and 100 K curves for $\mu_\perp$ for $\theta < \theta_{oct}$. This implies that as temperature falls, $\mu_\perp$ values may increase, decrease, or remain constant: the previously observed behaviour is for the higher principal moment to increase with decreasing temperature in this range and for the lower to decrease.

The behaviour of principal and average moments with ρ_4 is shown in Figure 4. Mean moments vary significantly with ρ_4 and, bearing in mind the relatively small θ dependence of $\bar{\mu}$(100 K), we can fix ρ_4 for $Tm(antip)_6I_3$ as 375 ± 40 cm^{-1}. This error estimate is made partly on the basis of Figure 4 being constructed for $\theta = 53°$ corresponding to a realistic estimate for the distortion parameter, as discussed later. Plots of principal moments have been included in Figure 4 to demonstrate how the temperature dependence of $\mu_\perp$, discussed earlier, can also depend on the ρ_4 value.

Figure 5 shows smooth, slight dependence of all

[9] M. Gerloch and D. J. Mackey, *J. Chem. Soc.* (*A*), 1971, 2605.

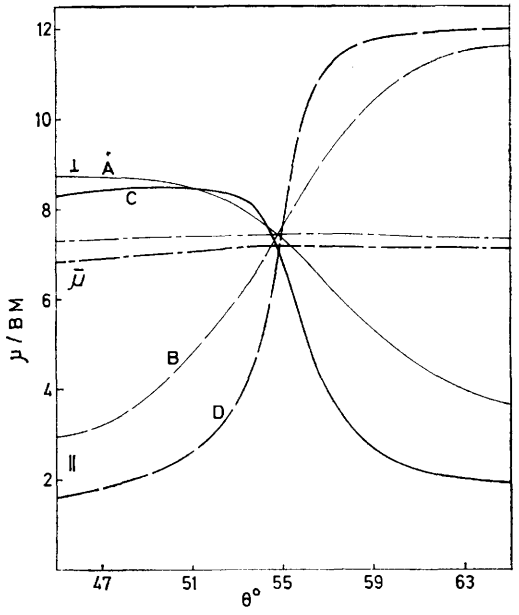

FIGURE 3 Principal and average magnetic moments at 300 (A, B) and 100 K (C, D) as functions of θ; ρ_2 1500, ρ_4 400, and ρ_6 200 cm^{-1}.

moments on ρ_6, all values decreasing with increasing ρ_6 values. The mean moments give no clear indication of the ρ_6 value in $Tm(antip)_6I_3$: for purposes of calculation we take ρ_6 as 200 $\pm$ 200 cm^{-1}.

Taking the aforementioned values for ρ_4 and ρ_6 and following the practice in earlier parts of this series, we have calculated anisotropies $\Delta\mu$ ($= \mu_\perp - \mu_\parallel$) as functions of θ for a series of ρ_2 values. Anisotropy values for ρ_2 1500 cm^{-1} are shown in Figure 6 in which experimental values for $Tm(antip)_6I_3$ indicate effective θ values for fit. As elsewhere in this series the θ value required for fitting the experimental anisotropy varies with temperature. In common with $Er(antip)_6I_3$, this temperature variation follows the scheme, θ^f(100 K) > θ^f(300 K) > θ^f(200 K): the temperature variation of θ^f is small, however.

Table 4 lists, for ρ_4 375, ρ_6 200 cm^{-1}, values of θ required to fit experimental $\Delta\mu$ values at 300, 200, and

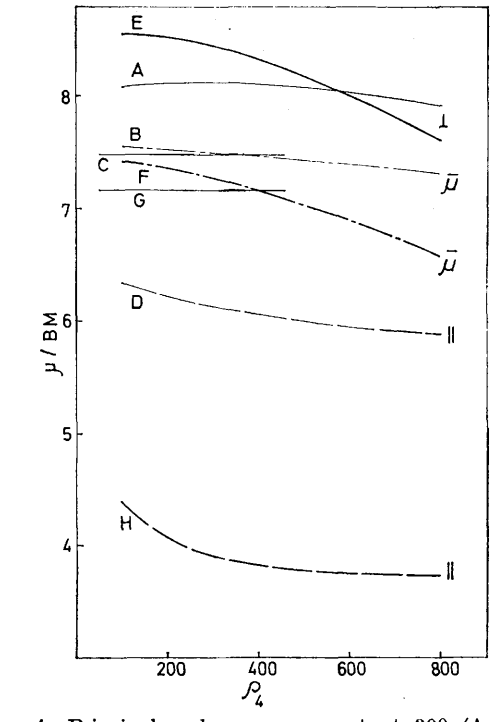

FIGURE 4 Principal and mean moment at 300 (A—D) and 100 K (E—H) as functions of ρ_4; ρ_2 1500, ρ_6 200 cm^{-1}, and θ = 53°. Experimental values for $Tm(antip)_6I_3$ are shown (C, G)

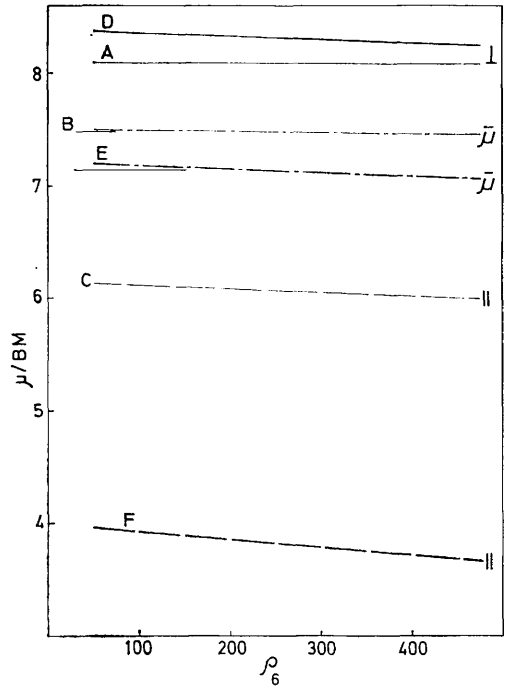

FIGURE 5 Principal and mean moments at 300 (A—C) and 100 K (D—F) as functions of ρ_6; ρ_2 1800, ρ_4 400 cm^{-1}, and θ = 53°. Experimental values for $Tm(antip)_6I_3$ are shown as horizontal lines

100 K for several values of ρ_2. The calculated mean moments associated with these ρ_2 and θ combinations are also shown: in all cases they agree with the experimental mean moments within 0·02 BM. For $\rho_2 \geqslant 1000$ cm^{-1}, values of $A_2^0\langle r^2\rangle$, [$= \frac{3}{2} \cdot \rho_3(3\cos^2\theta - 1)$], are independent of ρ_2, being *ca.* 200 $\pm$ 30 cm^{-1}: for ρ_2 500 cm^{-1}, $A_2^0\langle r^2\rangle$ takes a lower value, 170 $\pm$ 20 cm^{-1}. This differing behaviour for the lowest ρ_2 values has been noted in earlier parts of this series. For all ρ_2 values the trend in θ^f with temperature noted earlier is similar and is reflected in $A_2^0\langle r^2\rangle$ values. Such trends are incorporated in the estimated errors of $A_2^0\langle r^2\rangle$.

Conclusions.—The crystal-field radial parameters established by this work for $Tm(antip)_6I_3$ are $A_2^0\langle r^2\rangle$ 200 $\pm$ 30 cm^{-1}, ρ_4 375 $\pm$ 40 cm^{-1}; ρ_6 is not well defined. These values appear to be in line with those found for other members of the series. Trends which are emerging from these studies will be discussed fully on completion

of the series. Meanwhile we may compare the parameter values above with those obtained for Tm^{III} ions in two different environments. Englehardt and Figgis [10] studied powder susceptibilities of Tm^{3+} in $NaYF_4$, finding some evidence for magnetic concentration effects in the pure $NaTmF_4$ compound. Extrapolation of their

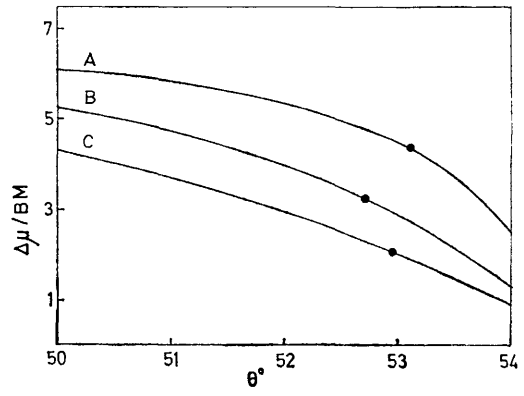

FIGURE 6 Example of fitting anisotropies of $Tm(antip)_6I_3$. Curves calculated with ρ_2 1500, ρ_4 375, ρ_6 200 cm^{-1}, at A 100, B 200, and C 300 K

TABLE 4

Calculated $\bar{\mu}$ and $A_2^0\langle r^2\rangle$ values for good fit to experimental $\Delta\mu$ values [experimental values: $\bar{\mu}$(300 K) 7·47, $\bar{\mu}$(200 K) 7·41, $\bar{\mu}$(100 K) 7·16 BM]

$\rho_4 = 375$, $\rho_6 = 200$ cm^{-1}.

T/K	$\theta°$	$A_2^0\langle r^2\rangle$/cm^{-1}	$\bar{\mu}$/BM
(*a*) ρ_2 500 cm^{-1}			
300	49·90	183	7·48
200	49·75	189	7·39
100	50·80	149	7·15
(*b*) ρ_2 1000 cm^{-1}			
300	52·13	195	7·48
200	51·84	217	7·40
100	52·45	171	7·16
(*c*) ρ_2 1500 cm^{-1}			
300	52·96	199	7·48
200	52·72	227	7·41
100	53·12	181	7·17
(*d*) ρ_2 2000 cm^{-1}			
300	53·36	204	7·48
200	53·20	229	7·40
100	53·48	186	7·18

results for various, Tm to Y ratios gave the value at 'infinite dilution': ρ_4 470 and ρ_6 204 cm^{-1}. Cooper *et al.*[11] studying octahedral TmN, report ρ_4 490 and ρ_6 9 cm^{-1}. There is evidently an order-of-magnitude agreement between these results and ours for ρ_4.

APPENDIX

As discussed in the Introduction, Runciman and Wybourne [6] have fitted experimental spectra of thulium sulphate and ethylsulphate to a four-parameter intermediate-coupling model but have only published their eigenvalues. We have repeated their calculation using Gruber and Conway's [4] expression for the diagonal inter-electron repulsion matrix elements and the spin–orbit coupling matrix of Spedding.[5] The 'best-fit' values of F_2, F_4, F_6, and ζ quoted by Runciman and Wybourne were: F_2 447·5, F_4 60·59, F_6 = 6·89, and ζ = 2575 cm^{-1}. Repeating their calculations (neglecting the Trees correction) we were unable to reproduce their reported eigenvalues. However, assuming a trivial printers' error such that we take ζ = 2755 cm^{-1}, we obtain perfect agreement with all levels except for the $^3H_4$. We find this at 5083 cm^{-1} above ground and not 5685 cm^{-1}, as reported: we therefore assume a printers' error in the second figure and a calculational rounding error in the last. The eigenvectors associated with the first seven levels (shown in Figure 1), calculated without a Trees correction are:

Label	Energy/cm^{-1}	Vector
$^3H_6$	0	$0·9949\|^3H_6\rangle + 0·1007\|^1I_6\rangle$
$^3H_4$	5083	$-0·2775\|^3H_4\rangle + 0·7701\|^3F_4\rangle + 0·5744\|^1G_4\rangle$
$^3H_5$	8607	$1·000\|^3H_5\rangle$
$^3F_4$	12,761	$-0·7291\|^3H_4\rangle - 0·5581\|^3F_4\rangle + 0·3961\|^1G_4\rangle$
$^3F_3$	14,527	$1·000\|^3F_3\rangle$
$^3F_2$	14,941	$0·8659\|^3F_2\rangle - 0·4771\|^1D_2\rangle - 0·1504\|^3P_2\rangle$
$^1G_4$	21,254	$0·7164\|^1G_4\rangle - 0·3089\|^3F_4\rangle + 0·6256\|^3H_4\rangle$

As in Part V,[1] we have calculated factors by which the term-reduced matrix elements of the crystal-field tensor operators must be multiplied. These are:

U_2 / U_4 / U_6	$^3H_6$	$^3H_4$	$^3H_5$	$^3F_4$	$^3F_3$	$^3F_2$
$^3H_6$	1·0101					
	0·9746					
	0·9858					
$^3H_4$	16·5713	−0·0901				
	−5·8804	1·0121				
	1·1758	−0·9195				
$^3H_5$	0·9949	−0·8988	1·0000			
	0·9949	0·7321	1·0000			
	0·9949	−1·2277	1·0000			
$^3F_4$	−0·5643	6·8979	0·3456	−1·3226		
	−0·3834	−1·4939	−1·1142	1·5448		
	−0·9521	−0·7181	0·0328	5·7453		
$^3F_3$	0	0·1814	1·0000	−1·7816	1·0000	
	0·9949	0·0331	1·0000	−2·3655	1·0000	
	0·9949	−0·4794	0	2·2226	1·0000	
$^3F_2$	0	−0·8119	0	15·4610	0·3449	1·6607
	−0·0602	−0·3583	0·9861	2·9861	1·2567	−1·9694
	0·9168	0·5684	0·9310	−0·9213	0	0

The importance of these correction factors can be seen by noting, for example, how $\langle^3H_4\|U_2\|^3H_4\rangle$ is to be taken as $-0·09\ \langle^3H\|U_2\|^3H\rangle$ *i.e.* negative and *ca.* 1/10th of the Russell–Saunders coupling value! Again, the off-diagonal element $\langle^3H_6\|U_2\|^3H_4\rangle$ is *ca.* 16 times larger than the term-reduced matrix element $\langle^3H\|U_2\|^3H\rangle$.

In parenthesis we note that $\langle^3H_5\|U_6\|^3F_3\rangle$ vanishes because the 6-*j* symbol $\begin{Bmatrix}5 & 5 & 1\\ 3 & 3 & 6\end{Bmatrix}$ vanishes.

There is an element of illogicality in our theoretical approach in that we have corrected the basis orbitals used for the crystal-field calculations as described here, but still use the pure Russell–Saunders kets for calculating matrix elements of the magnetic moment operators. The reasons for this approach are two-fold, being concerned with calculational simplicity on the one hand and reasonable neglect on the other. Thus all calculations are performed in our programme within the simply defined kets of the pure Russell–Saunders states. The intermediate coupling correction to these kets is implicit in that we use the

[10] L. M. Engelhardt and B. N. Figgis, *J. Chem. Soc.* (*A*), 1970, 415.

[11] B. R. Cooper, I. S. Jacobs, R. C. Fedder, J. S. Kouvel, and D. P. Schumacher, *J. Appl. Phys.*, 1966, **37**, 1384.

matrices above to correct the crystal-field reduced matrix elements. Thus, the eigenvectors produced by diagonalization of the crystal-field perturbation are still linear combinations of the pure Russell–Saunders kets originally used as a basis. This is obviously necessary to avoid working with impossibly large basis sets. We should therefore use correction factors for magnetic moment matrix elements in a similar way to those used for the $U(k)$ matrices. This is tedious and has not been done for the following reasons.

We have compared Landé g factors calculated for the pure Russell–Saunders states by the usual relation:

$$g = 1 + \frac{J(J+1) - L(L+1) + S(S+1)}{2J(J+1)}$$

with those calculated using this expression weighted according to the vector coefficient given at the beginning of this Appendix and corresponding tables for the other f ions. They are equal within *ca.* 1—2% for the lowest state throughout the lanthanide series. Magnetic moments predominantly involve crystal-field components of the ground state, the admixture with other states being fairly small. This is evidenced by our ability to terminate basis sets in these calculations after the first two states, or even almost after the first one. In other words higher states have rather little effect on moments. The intermediate coupling affects the way the crystal-field splits up the lowest state and hence is important magnetically in determining energies of the ground-state components. But as far as magnetic moments are concerned, intermediate coupling is not important for the eigenvectors of these lower states, as evidenced by the g-value calculation discussed.

[1/1331 *Received, July 30th,* 1971]